nature biomedical engineering

Article

https://doi.org/10.1038/s41551-023-01015-3

# Rapid single-cell physical phenotyping of mechanically dissociated tissue biopsies

In the format provided by the authors and unedited

## CONTENTS

## 1. Supplementary Figures



## 2. Supplementary Tables

## Supplementary Figures

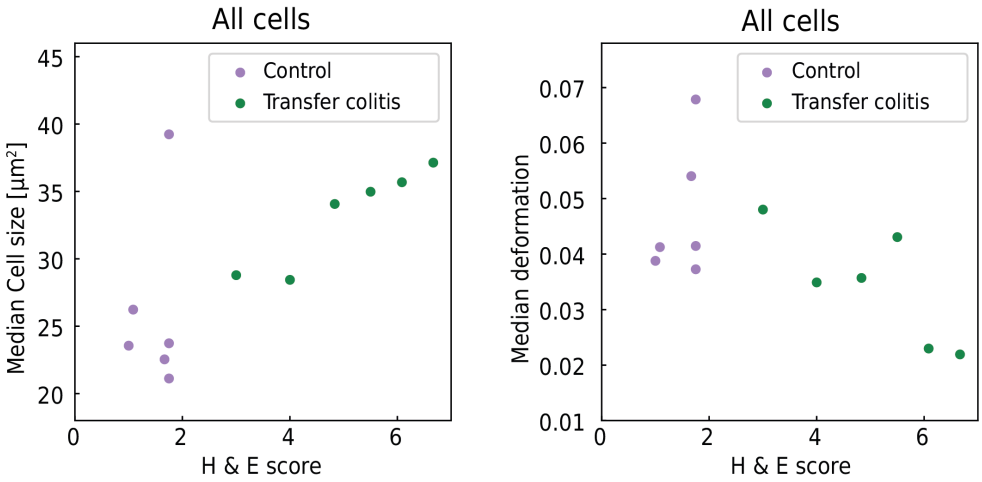


**Supplementary Fig. 1 | Correlation of physical phenotype parameters obtained using RT-FDC and histopathology scoring of mouse transfer colitis samples.** Plot of Haematoxylin & Eosin (H&E) scoring vs median cell size (left) and deformation (right) of all cells measured. Transfer colitis samples are shown in green, control (healthy) samples are shown in purple.

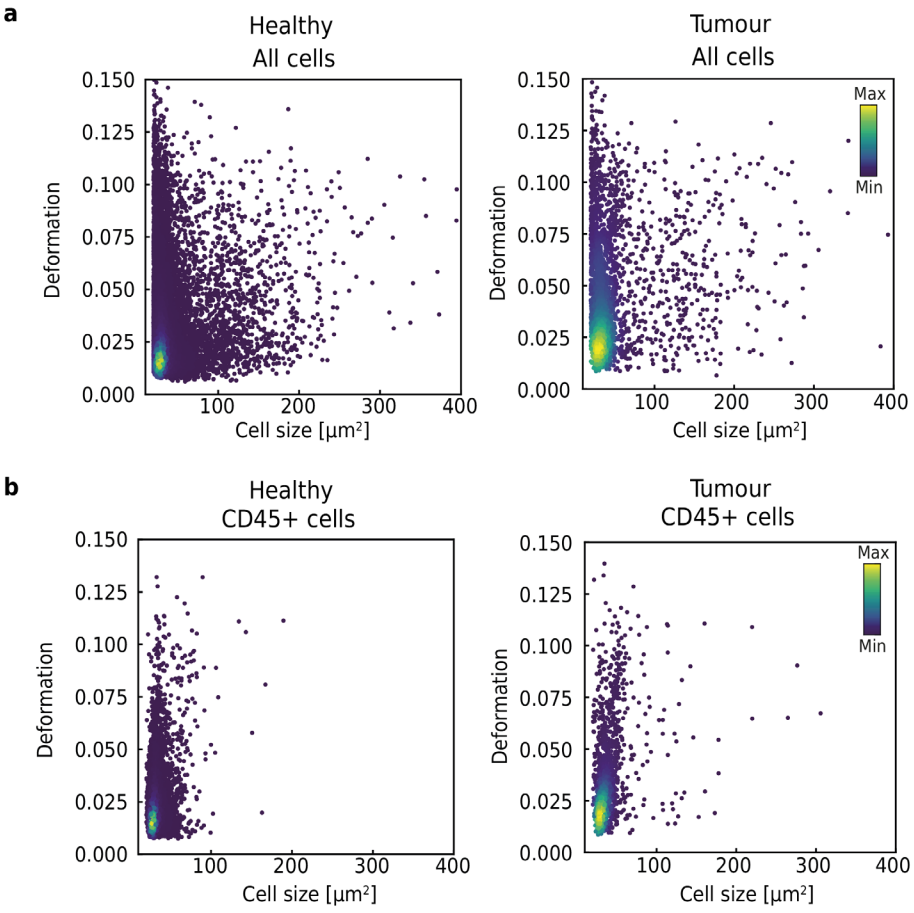


c

| | Mean | STD |
|---|---|---|
| debris / all events < 60µm² | 89.6% | 10.5% |
| CD45+ cells / total cells < 60µm² | 57.2% | 19.0% |

**Supplementary Fig. 2 | Exclusion of small cells from the analysis of healthy vs tumour murine colon samples. a,** Representative RT-FDC scatter plots of deformation vs cell size, showing cells isolated from tumour or healthy murine colon samples. **b,** Representative scatter plots of CD45 positive cells (a marker of leukocytes), showing that a high percentage of these cells are less than 60 µm² in size. These cells were excluded from the analysis. **c,** The percentage of debris in events less than 60 µm² in size and the percentage of CD45 positive cells, calculated as mean and standard deviation of all measured samples.

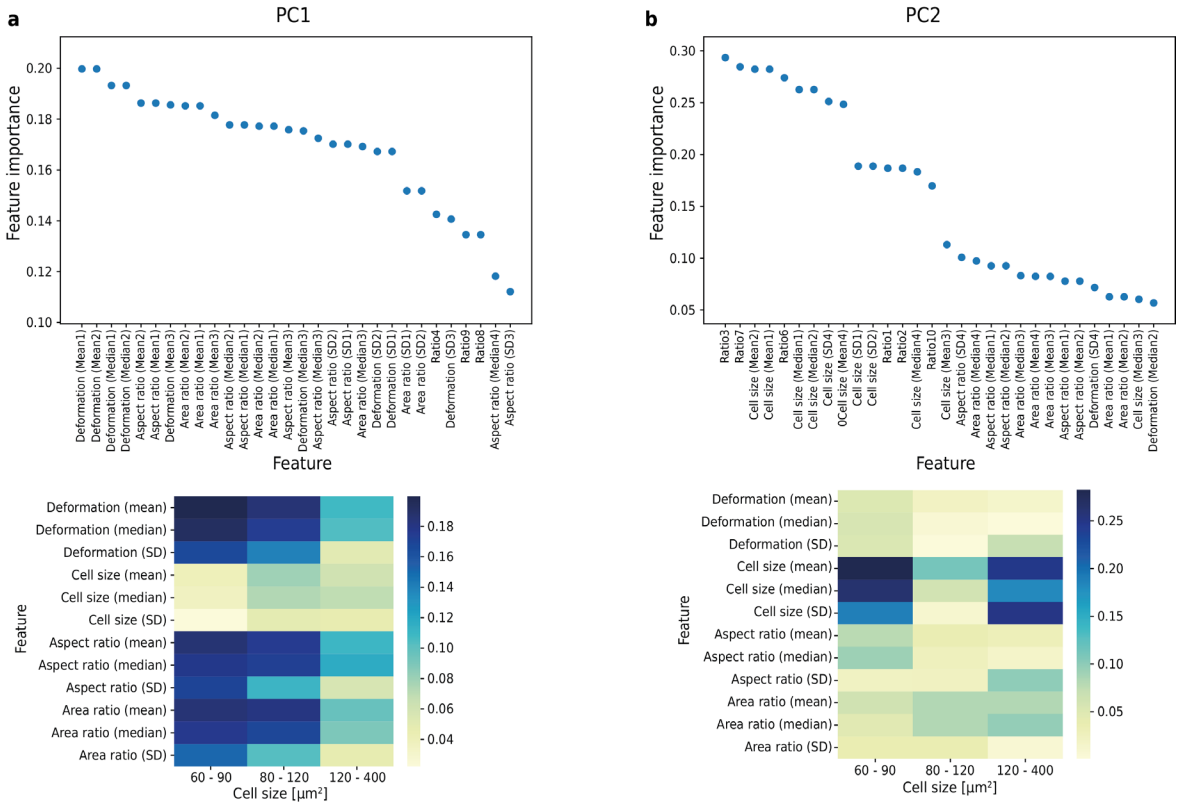


**Supplementary Fig. 3 | Principal component feature importance for mouse tumours.** PCA was performed on a total of 36 parameters; 12 parameters (y axis) for 3 cell size categories (x axis). **a,** Relative feature importance for PC1 and **b,** PC2. SD: standard deviation. The number at the end of each feature label describes which bin of cell sizes it corresponds to; 1: 60-90; 2: 80-120; 3: 120-400 µm$^2$.

**a**

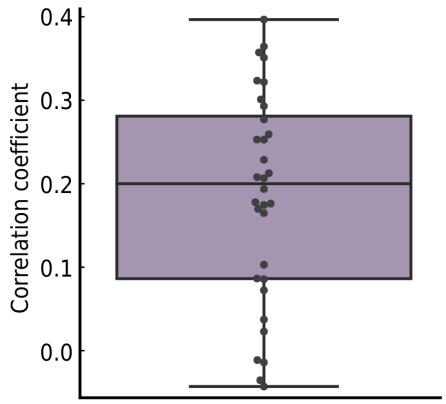


**b**

| Correlation coefficients | Mean area and mean deformation | Median area and median deformation |
|---|---|---|
| Cells 60 - 90 µm² | 0.078 | 0.084 |
| Cells 80 - 120 µm² | 0.064 | 0.174 |
| Cells 120 - 400 µm² | 0.001 | -0.008 |

**Supplementary Fig. 4 | Correlation of deformation and cell size in murine healthy and tumour samples**. a, Pearson's correlation coefficients for deformation and area; each point corresponds to one murine sample and b, table showing Pearson's correlation coefficients for the statistical means and medians of area and deformation, divided into the three cell size categories used for the principal component analysis. The box plot extends from the 25$^{th}$ to the 75$^{th}$ percentile with a line at the median; whiskers span 1.5x the interquartile range.

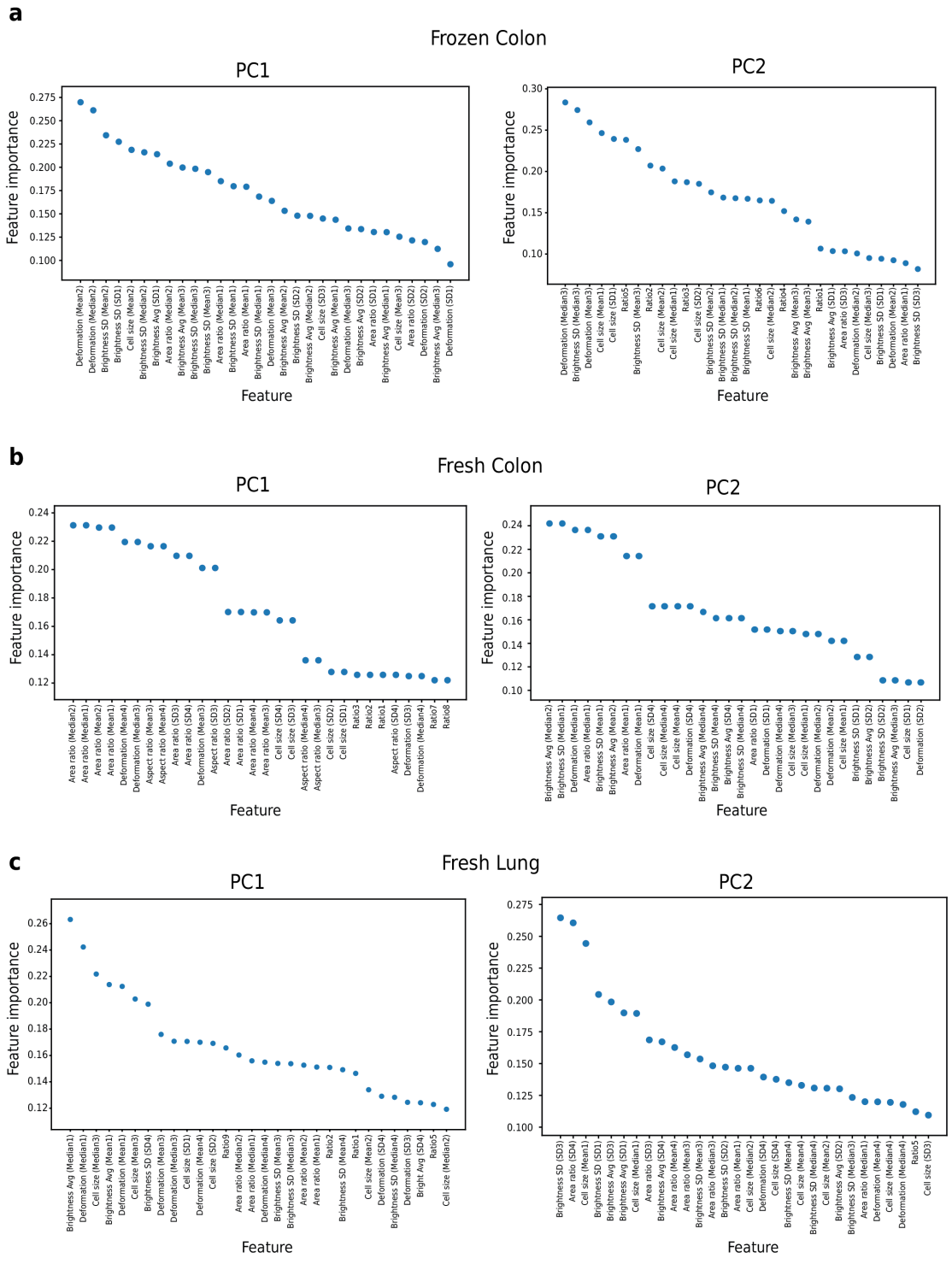


**Supplementary Fig. 5 | Principal component feature importance for human biopsy samples.** Relative feature importance for PC1 and PC2 for **a,** frozen colon biopsy samples, **b,** fresh colon biopsy samples, **c,** fresh lung biopsy samples. The number at the end of each feature label describes which bin of cell sizes it corresponds to (the bins are given in Fig. 5). Frozen colon: 1: 20-60; 2: 60-100; 3: 100-600 μm$^2$. Fresh colon: i.e. 1: 20-50; 2: 50-600 μm$^2$. Fresh Lung: 1: 20-60; 2: 60-100; 3: 100-200. 4: 200-600 μm$^2$. SD: standard deviation.

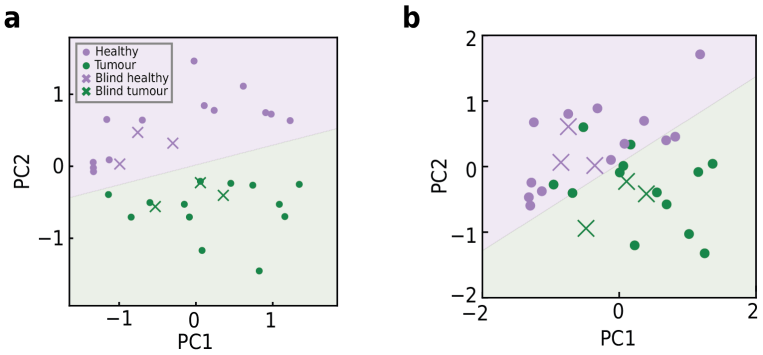


**Supplementary Fig. 6 | Testing the performance of healthy vs tumour classification of frozen human colon samples. a,** PCA and logistic regression including the full set of 45 parameters as input for PCA; **b,** PCA and logistic regression after excluding 3 parameters (deformation mean, median and SD for cells larger than 100 μm$^2$).

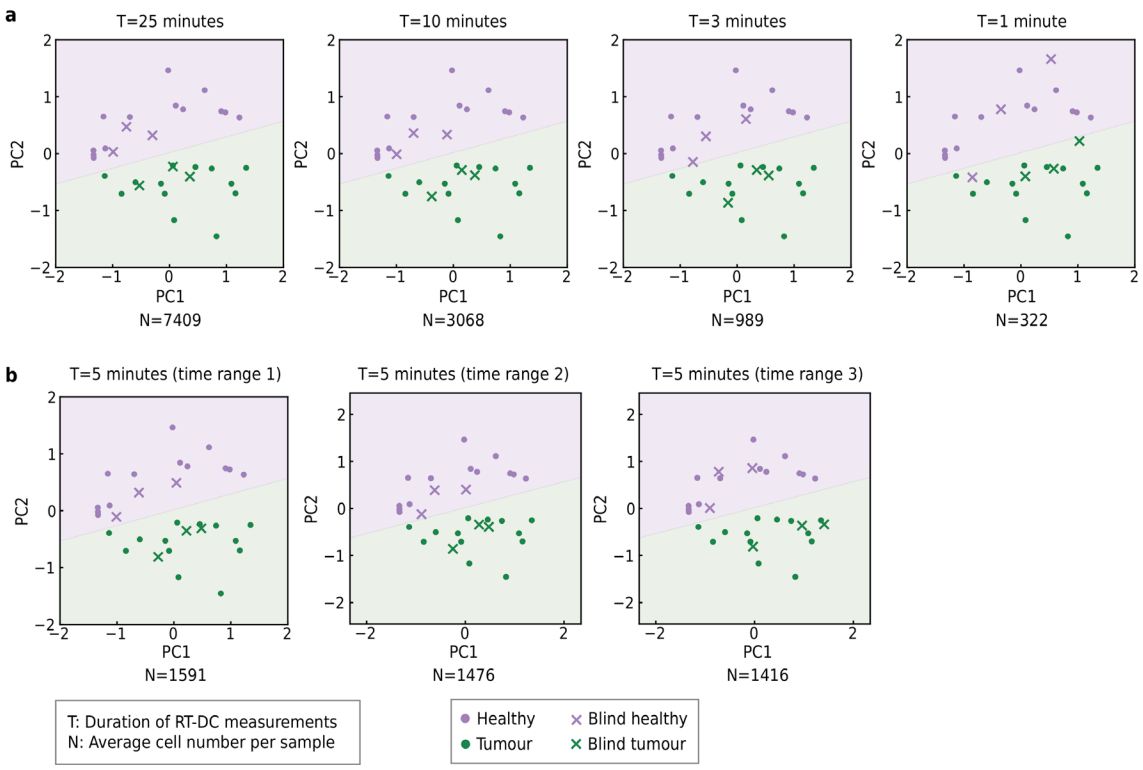


**Supplementary Fig. 7 | Testing the performance of healthy vs tumour classification on reduced data from frozen human colon samples. a,** Logistic regression was performed on the PCA (shown by the linear divide in the PCA plot) and used to predict the classification of six blind samples (shown as crosses). From left to right, the amount of data used for classification decreases (the plots correspond to experiment durations of T = 25, 10, 3 and 1 minute). The average cell numbers analysed for a sample are shown below each plot (N). Classification was correct for experiments lasting 3 minutes or longer; data yielded by a one-minute experiment was insufficient for 100% correct classification of healthy vs tumour samples. **b,** PCA plots performed using approximately 1500 cells (or an equivalent of 5 minutes of measurement) extracted from different time points of longer RT-FDC measurements.

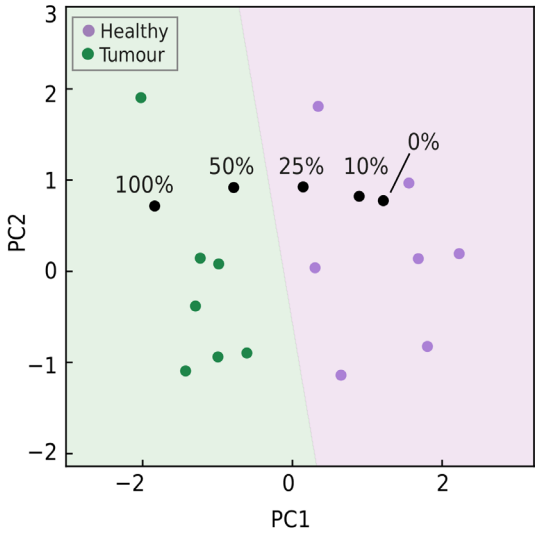


**Supplementary Fig. 8 | Testing of the performance of logistic regression on mixed samples consisting of different ratios of tumour and healthy lung biopsy samples.** The percentages indicate the percentage of the volume of the dissociated tumour sample in the total sample volume. The pure tumour sample and the sample with 50% tumour content were classified as tumour, while 25%, 10% and 0% of tumour content resulted in a classification in the “healthy” category.

## Supplementary Tables

**Supplementary Table 1 |** Standard dissociation protocols used for each organ; *n* indicates the number of biological repeats per tissue.

| Tissue | Dissociation procedure | *n* |
|---|---|---|
| **Colon** | Miltenyi Biotec Lamina Propria Dissociation Kit | 4 |
| **Small Intestine** | Miltenyi Biotec Lamina Propria Dissociation Kit | 4 |
| **Lung** | Miltenyi Biotec Lung Dissociation kit | 4 |
| **Liver** | Miltenyi Biotec Liver Dissociation Kit or Collagenase/Dispase enzymatic cocktail | 4 |
| **Stomach** | Ruiz et al 2012[1] | 3 |
| **Kidney** | Valente et al 2011[2] | 3 |
| **Pancreas** | Epshtein et al 2017[3] | 3 |
| **Thymus** | Mash tissue between frosted ends of two microscope slides | 4 |
| **Mesenteric Lymph Node** | Mash tissue between frosted ends of two microscope slides | 4 |
| **Spleen** | Mash tissue between frosted ends of two microscope slides | 4 |

**Supplementary Table 2 |** Mouse organs with the corresponding tissue grinder protocols used for mechanical dissociation, together with the microfluidic chip size used for RT-FDC measurement; *n* indicates the number of biological repeats per tissue.

| Tissue | Tissue grinder protocol | Microfluidic chip size | *n* |
|---|---|---|---|
| **Colon** | Colon | 20 µm | 4 |
| **Small Intestine** | Intestine | 20 µm | 4 |
| **Lung** | Lung standard | 30 µm | 4 |
| **Liver** | Liver standard | 30 µm & 40 µm | 4 |
| **Kidney** | Medium | 30 µm | 5 |
| **Pancreas** | Soft | 30 µm | 4 |
| **Thymus** | Thymus Soft | 30 µm | 4 |
| **Mesenteric Lymph Node** | Lymph nodes standard | 30 µm | 4 |
| **Spleen** | Thymus Soft | 30 µm | 5 |
| **Stomach** | Intestine | 30 µm | 4 |
| **Human tumour** | Human Tumour | 20 µm | - |

**Supplementary Table 3 |** Parameters derived from cell images in real-time during an RT-FDC measurement.

| RT-FDC parameters | Description |
|---|---|
| **Area (cell size; µm²)** | The projected cross-sectional area of the cells is obtained from the number of pixels within the boundary of the cell, defined by the contour |
| ***Bounding box size x* and *y*** | A bounding box around the whole cell defines its length in x and y direction |
| **Aspect ratio** | Ratio between object's length (x) and height (y) |
| **Circularity** | Parameter that quantifies the deviation from a circular cross-section, by relating area (*A*) to the perimeter (*P*) of an object based on $C = \frac{2\sqrt{\pi A}}{P}$ |
| **Deformation** | $\frac{1 - 2\sqrt{\pi A}}{P}$ |
| **Inertia ratio** | Ratio of the second moment of area over the y- and x-axis of the contour. |
| **Area ratio** | Ratio between the area of the convex hull and the area of the contour |
| **Brightness [a.u.]** | Mean of all pixel intensities inside the contour |
| **Standard deviation of brightness** | Standard deviation of the brightness of pixels inside the contour |
| **X position** | Position along the flow axis in the field of view. |
| **Y position** | Position perpendicular to flow axis in the field view |
| **Volume** | The apparent volume based on the assumption of rotational symmetry over the flow axis. |
| **Elastic modulus (Young's Modulus)** | Describes cell stiffness, based on assumptions of a model |
| **Fluorescence area of peak [µs]** | Area of the fluorescence intensity peak |
| **Fluorescence maximum [a.u.]** | Maximum fluorescence intensity |
| **Fluorescence width [µs]** | Full width at half-maximum; used to identify the sub-cellular distribution of fluorescence marker |

**Supplementary Table 4 |** Antibodies and fluorescent probe solutions used with the corresponding dilutions.

| | Reactivity | Dilution | Clone | Cat. No | Company |
|---|---|---|---|---|---|
| CD326 (EpCAM) Alexa Fluor® 488 | Human | 1 in 100 | 9C4 | 324210 | BioLegend |
| CD31(PECAM-1) APC | Human | 5µl/reaction | WM59 | 303115 | BioLegend |
| CD45 PE | Human | 1 in 500 | HI30 | 304008 | BioLegend |
| CD326 (EpCAM) FITC | Human | 1 in 100 | 9C4 | 324203 | BioLegend |
| CD45 Alexa Fluor® 700 | Human | 5µl/reaction | HI30 | 304024 | BioLegend |
| CD45 Alexa Fluor® 700 | Mouse | 1 in 1000 | 30-F11 | 103128 | BioLegend |
| CD326 (EpCAM) Alexa Fluor® 488 | Mouse | 1 in 200 | G8.8 | 118210 | BioLegend |
| CD45 FITC | Mouse | 1 in 800 | 30-F11 | 11-0451-82 | Thermo Fischer Scientific |
| CD326 (EpCAM) APC | Mouse | 1 in 500 | G8.8 | 17-5791-82 | Thermo Fischer Scientific |
| CD31 (PECAM-1) PE | Mouse | 1 in 250 | 390 | 12-0311-82 | Thermo Fischer Scientific |
| DRAQ5™ | - | 5µl/reaction | - | 65-0880-92 | Thermo Fischer Scientific |
| Propidium Iodide | - | 1 in 2000 | - | P1304MP | Thermo Fischer Scientific |
| 7-AAD Viability Solution | - | 5µl/reaction | - | 420404 | Thermo Fischer Scientific |

**Supplementary Table 5 |** Pathological information and stromal content evaluation of frozen human colon biopsy samples. sTILs: stromal tumour infiltrating lymphocytes (scored as percent of total tumour stroma occupied by tumour infiltrating lymphocytes). M: Male, F: Female. Samples were frozen prior to mechanical dissociation and analysis with RT-FDC.

| Sample Number | Sex | Age | Diagnosis | Stromal Content (%) | Stroma Appearance | sTILs (%) | Localization of Biopsy |
|---|---|---|---|---|---|---|---|
| S1_Colon_Frozen | M | 81 | Colonic Adenocarcinoma | 10 | Fibrous | 25 | Colon Transversum |
| S3_Colon_Frozen | M | 77 | Colonic Adenocarcinoma | 20 | Fibrous | 5 | Colon Sigmoidoum |
| S4_Colon_Frozen | M | 61 | Colonic Adenocarcinoma | 5 | Fibrous | 3 | Colon Sigmoidoum |
| S5_Colon_Frozen | M | 71 | Colonic Adenocarcinoma | 30 | Fibrous | 3 | Colon Ascendens |
| S6_Colon_Frozen | M | 84 | Colonic Adenocarcinoma | 40 | Fibrous | 40 | Colon Ascendens |
| S7_Colon_Frozen | M | 83 | Rectal Adenocarcinoma | 98 | Fibrous | 2 | Rectum |
| S8_Colon_Frozen | F | 57 | Colonic Adenocarcinoma | 30 | Leiomyomatous | 15 | Rectum |
| S9_Colon_Frozen | M | 69 | Colonic Adenocarcinoma | 35 | Chondromyxoid | 3 | Colon Sigmoidoum |
| S11_Colon_Frozen | M | 85 | Rectal Adenocarcinoma | 80 | Chondromyxoid | 3 | Rectum |
| S12_Colon_Frozen | M | 86 | Colonic Adenocarcinoma | 60 | Leiomyomatous | 40 | Colon Transversum |
| S13_Colon_Frozen | M | 73 | Colonic Adenocarcinoma | 25 | Fibrous | 30 | Colon Ascendens |
| S14_Colon_Frozen | M | 69 | Colonic Adenocarcinoma | 20 | Leiomyomatous | 15 | Colon Transversum |
| S16_Colon_Frozen | M | 88 | Colonic Adenocarcinoma | 15 | Fibrous | 5 | Colon Ascendens |

**Supplementary Table 6 |** Pathological information and stromal content evaluation of frozen human colon biopsy samples. sTILs: stromal tumour infiltrating lymphocytes (scored as percent of total tumour stroma occupied by tumour infiltrating lymphocytes). M: Male, F: Female. Samples were immediately processed with the tissue grinder and analysed with RT-FDC without prior freezing. Blue shaded samples were used as blind samples.

| Sample Number | Sex | Age | Diagnosis | Stromal Content (%) | Stroma Appearance | sTILs (%) | Localization of Biopsy |
|---|---|---|---|---|---|---|---|
| S1_Colon_Fresh | F | 62 | Colonic Adenocarcinoma | 40 | Myxoid | 15 | Colon |
| S2_Colon_Fresh | M | 76 | Colonic Adenocarcinoma | 30 | Fibrous | 15 | Colon |
| S3_Colon_Fresh | M | 81 | Colonic Adenocarcinoma | 10 | Fibrous | 25 | Colon |
| S4_Colon_Fresh | M | 85 | Colonic Adenocarcinoma | 25 | Leiomyomatous | 15 | Colon |
| S5_Colon_Fresh | F | 68 | Colonic Adenocarcinoma | 15 | Fibrous | 25 | Sigma-Colon |
| S6_Colon_Fresh | M | 83 | Adenocarcinoma | 10 | Fibrous | 5 | Colon |
| S7_Colon_Fresh | M | 60 | Colonic Adenocarcinoma | 25 | Fibrous | 35 | Colon |
| S8_Colon_Fresh | M | 61 | Colonic Adenocarcinoma | 45 | Fibrous | 25 | Colon |
| S9_Colon_Fresh | F | 61 | Colonic Adenocarcinoma | 15 | Fibrous | 10 | Colon |
| S10_Colon_Fresh | F | 69 | Colonic Adenocarcinoma | 10 | Fibrous | 5 | Colon |
| S11_Colon_Fresh | F | 79 | Colonic Adenocarcinoma | 25 | Fibrous | 7 | Colon |
| S12_Colon_Fresh | F | 81 | Colonic Adenoma - high grade | 20 | Fibrous | 60 | Colon |
| S13_Colon_Fresh | F | 69 | Colonic Adenocarcinoma | 5 | Fibrous | 5 | Colon |
| S14_Colon_Fresh | F | 70 | Colonic Adenocarcinoma | 5 | Fibrous | 25 | Colon |
| S15_Colon_Fresh | F | 83 | Colonic Adenocarcinoma | 5 | Fibrous | 50 | Colon |
| S16_Colon_Fresh | M | 77 | Colonic Adenocarcinoma | 10 | Fibrous | 15 | Colon |

**Supplementary Table 7 |** Histopathological evaluation of frozen human colon biopsy samples. T: tumour classification (ranges from T1 to T4). Grade 1: tumour cells look like healthy cells. Grade 2: tumour cells are somewhat abnormal. Grade 3: tumour cells and tissue look very abnormal. Grade 4: tumour cells are very abnormal. N: lymph node classification that assess infiltration of locoregional lymph nodes by the subsequent carcinoma/tumour (0=no lymph node metastases) The numbers in parentheses reflect the number of infiltrated lymph nodes (before the slash) and the number of evaluated lymph nodes (after the slash). L: Lymphovascular invasion; V: Blood Vessel invasion; Pn: perineural invasion; 0 means no invasion present, 1= invasion present; R= resection status; R0 = tumour is completely resected. NOS: not otherwise specified.

| Sample Number | Histology | pT-Stage | pN-Stage | Grading | L | V | Pn | R |
|---|---|---|---|---|---|---|---|---|
| S1_Colon_Frozen | Intestinal Adenocarcinoma - Mucinous | pT2a | pN0 (0/21) | G2 | 0 | 0 | 0 | 0 |
| S3_Colon_Frozen | Intestinal Adenocarcinoma - NOS | pT3c | pN0 (0/20) | G2 | 0 | 0 | 0 | 0 |
| S4_Colon_Frozen | Intestinal Adenocarcinoma - NOS | pT3b | pN0 (0/33) | G2 | 0 | 0 | 0 | 0 |
| S5_Colon_Frozen | Intestinal Adenocarcinoma - NOS | pT3b | pN0 (0/17) | G3 | 0 | 0 | 0 | 0 |
| S6_Colon_Frozen | Intestinal Adenocarcinoma - Mucinous | pT3c | pN2b (10/12) | G3 | 1 | 1 | 0 | 0 |
| S7_Colon_Frozen | Intestinal Adenocarcinoma - NOS | ypT2a | ypN1b (2/23) | G2 | 0 | 0 | 0 | 0 |
| S8_Colon_Frozen | Intestinal Adenocarcinoma - NOS | pT2a | pN0 (0/36) | G2 | 0 | 0 | 0 | 0 |
| S9_Colon_Frozen | Intestinal Adenocarcinoma - NOS | pT3b | pN2a (4/20) | G3 | 0 | 0 | 1 | 0 |
| S11_Colon_Frozen | Intestinal Adenocarcinoma - NOS | ypT3b | pN0 (0/33) | G2 | 0 | 0 | 0 | 0 |
| S12_Colon_Frozen | Intestinal Adenocarcinoma - NOS | pT2b | pN1a (1/24) | G3 | 1 | 1 | 0 | 0 |
| S13_Colon_Frozen | Intestinal Adenocarcinoma - NOS | pT2b | pN0 (0/42) | G3 | 0 | 0 | 0 | 0 |
| S14_Colon_Frozen | Intestinal Adenocarcinoma - NOS | pT4b | pN0 (0/18) | G2 | 1 | 0 | 0 | 0 |
| S16_Colon_Frozen | Intestinal Adenocarcinoma - NOS | pT4a | pN2b (4/17) | G3 | 1 | 0 | 0 | 0 |

**Supplementary Table 8 |** Histopathological evaluation of fresh human colon biopsy samples. T: tumour classification (ranges from T1 to T4). Grade 1: tumour cells look like healthy cells. Grade 2: tumour cells are somewhat abnormal. Grade 3: tumour cells and tissue look very abnormal. Grade 4: tumour cells are very abnormal. N: lymph node classification that assess infiltration of locoregional lymph nodes by the subsequent carcinoma/tumour (0=no lymph node metastases) The numbers in parentheses reflect the number of infiltrated lymph nodes (before the slash) and the number of evaluated lymph nodes (after the slash). L: Lymphovascular invasion; V: Blood Vessel invasion; Pn: perineural invasion; 0 means no invasion present, 1= invasion present; R= resection status; R0 = tumour is completely resected. NOS: not otherwise specified. Blue shaded samples were used as blind samples.

| Sample Number | Histology | pT-Stage | pN-Stage | Grading | L | V | Pn | R |
|---|---|---|---|---|---|---|---|---|
| S1_Colon_Fresh | Intestinal Adenocarcinoma - NOS | pT4a | pN2a (6/30) | G3 | 1 | 1 | 1 | 0 |
| S2_Colon_Fresh | Intestinal Adenocarcinoma - NOS | pT3a | pN0 (0/29) | G2 | 0 | 0 | 0 | 0 |
| S3_Colon_Fresh | Intestinal Adenocarcinoma - NOS | pT3b | pN1b (3/28) | G2 | 1 | 0 | 0 | 0 |
| S4_Colon_Fresh | Intestinal Adenocarcinoma - NOS | pT3a | pN0 (0/12) | G2 | 0 | 0 | 0 | 0 |
| S5_Colon_Fresh | Intestinal Adenocarcinoma - NOS | pT3a | pN2b (7/16) | G3 | 1 | 1 | 1 | 0 |
| S6_Colon_Fresh | Intestinal Adenocarcinoma - NOS | pT3c | pN0 (0/16) | G2 | 0 | 0 | 0 | 0 |
| S7_Colon_Fresh | Intestinal Adenocarcinoma - Mucinous | pT3c | pN1a (1/22) | G3 | 0 | 0 | 0 | 0 |
| S8_Colon_Fresh | Intestinal Adenocarcinoma - NOS | pT4a | pN0 (0/27) | G3 | 0 | 0 | 0 | 0 |
| S9_Colon_Fresh | Intestinal Adenocarcinoma - NOS | pT2 | pN1a (1/18) | G3 | 0 | 0 | 0 | 0 |
| S10_Colon_Fresh | Intestinal Adenocarcinoma - Mucinous | pT3c | pN0 (0/17) | G3 | 0 | 0 | 0 | 0 |
| S11_Colon_Fresh | Intestinal Adenocarcinoma - NOS | pT3d | pN0 (0/33) | G2 | 0 | 0 | 0 | 0 |
| S13_Colon_Fresh | Colonic Adenoma - high grade | N/A | N/A | high grade | N/A | N/A | N/A | N/A |
| S14_Colon_Fresh | Intestinal Adenocarcinoma - Mucinous/Gastric Type | pT4a | pN1a (1/33) | G3 | 0 | 0 | 1 | 0 |
| S15_Colon_Fresh | Intestinal Adenocarcinoma - Medullary Type | pT3d | pN1a (1/32) | G3 | 1 | 0 | 0 | 0 |
| S16_Colon_Fresh | Intestinal Adenocarcinoma - NOS | pT2b | pN0 (0/23) | G2 | 0 | 0 | 0 | 0 |

**Supplementary Table 9 |** Pathological information and stromal content evaluation of fresh human lung biopsy samples. sTILs: stromal tumour infiltrating lymphocytes (scored as percent of total tumour stroma occupied by tumour infiltrating lymphocytes). M: Male, F: Female. NSCLC: non-small cell lung cancer; SCLC: small cell lung cancer. Samples were immediately processed with the tissue grinder and analysed with RT-FDC without prior freezing. Blue shaded samples were used as blind samples.

| Sample Number | Sex | Age | Diagnosis | Stromal Content (%) | Stroma Appearance | sTILs (%) | Localization of Biopsy |
|---|---|---|---|---|---|---|---|
| S1_Lung_Fresh | M | 71 | NSCLC - Adenocarcinoma | 25 | Fibrous | 100 | Pulmonary Lymph Node |
| S2_Lung_Fresh | M | 85 | NSCLC - Squamous Cell Carcinoma | 15 | Chondromyxoid | 35 | Lung |
| S4_Lung_Fresh | M | 60 | NSCLC - Adenosquamous Carcinoma | 5 | Fibrous | 1 | Lung |
| S5_Lung_Fresh | M | 81 | NSCLC - Squamous Cell Carcinoma | 25 | Chondromyxoid | 15 | Lung |
| S6_Lung_Fresh | M | 64 | NSCLC - Adenocarcinoma | 50 | Fibrous | 50 | Lung |
| S7_Lung_Fresh | M | 72 | NSCLC - Squamous Cell Carcinoma | 10 | Fibrous | 1 | Lung |
| S8_Lung_Fresh | F | 76 | SCLC | 1 | Fibrous | 15 | Lung |
| S9_Lung_Fresh | M | 70 | NSCLC - Squamous Cell Carcinoma | 30 | Fibrous | 3 | Lung |

**Supplementary Table 10 |** Histopathological evaluation of fresh human lung biopsy samples. T: tumour classification (ranges from T1 to T4). Grade 1: tumour cells look like healthy cells. Grade 2: tumour cells are somewhat abnormal. Grade 3: tumour cells and tissue look very abnormal. Grade 4: tumour cells are very abnormal. N: lymph node classification that assess infiltration of locoregional lymph nodes by the subsequent carcinoma/tumour (0=no lymph node metastases) The numbers in parentheses reflect the number of infiltrated lymph nodes (before the slash) and the number of evaluated lymph nodes (after the slash). L: Lymphovascular invasion; V: Blood Vessel invasion; Pn: perineural invasion; 0 means no invasion present, 1= invasion present; R= resection status; R0 = tumour is completely resected. Blue shaded samples were used as blind samples.

| Sample Number | Histology | pT-Stage | pN-Stage | Grading | L | V | Pn | R |
|---|---|---|---|---|---|---|---|---|
| S1_Lung_Fresh | Primary Pulmonary Adenocarcinoma - Solid Type | TX | pN2 (2/10) | G3 | 1 | 0 | 0 | 0 |
| S2_Lung_Fresh | Primary Pulmonary Squamous Cell Carcinoma | pT3 | pN0 (0/56) | G2 | 1 | 0 | 0 | 0 |
| S4_Lung_Fresh | Primary Pulmonary Adenosquamous Carcinoma | pT4 | pN1 (1/10) | G3 | 1 | 0 | 1 | 0 |
| S5_Lung_Fresh | Primary Pulmonary Squamous Cell Carcinoma | pT2b | pN0 (0/34) | G3 | 0 | 0 | 0 | 0 |
| S6_Lung_Fresh | Primary Pulmonary Adenocarcinoma - Lepidic Type | pT1c | pN0 (0/29) | G1 | 0 | 0 | 1 | 0 |
| S7_Lung_Fresh | Primary Pulmonary Squamous Cell Carcinoma | pT4 | pN0 (0/18) | G3 | 0 | 0 | 0 | 0 |
| S8_Lung_Fresh | Small Cell Neuroendocrine Carcinoma | pT1c | pN0 (0/18) | G3 | 0 | 0 | 0 | 0 |
| S9_Lung_Fresh | NSCLC - Squamous Cell Carcinoma | pT1c | N/A | G3 | 0 | 0 | 0 | 0 |

**Supplementary Table 11 |** Deformability Cytometry Open Repository (DCOR) dataset identifiers[4].

| Dataset name | DCOR Identifier |
|---|---|
| Figure 2 - Liver, colon, kidney data | https://dcor.mpl.mpg.de/defc199e-d465-4254-9b65-973408f7843a |
| Figure 3 - Control group (murine colon samples) | https://dcor.mpl.mpg.de/d2eb46c2-92d4-41a8-aed0-1b77c6a43ba6 |
| Figure 3 - Transfer colitis (murine colon samples) | https://dcor.mpl.mpg.de/04c95441-311e-47bf-b122-01d9e6c5d1f4 |
| Figure 4 - Control group (murine colon samples) | https://dcor.mpl.mpg.de/35af55de-9f5c-4a57-8b9b-55eefade4613 |
| Figure 4 - Tumour (murine colon samples) | https://dcor.mpl.mpg.de/0f1544ae-00d4-4e2b-b413-737aa034eb3a |
| Figure 5 - Frozen human colon samples – healthy | https://dcor.mpl.mpg.de/b3512170-77d8-4c8e-8e52-b407f841e57e |
| Figure 5 - Frozen human colon samples – tumour | https://dcor.mpl.mpg.de/578beb51-885b-443f-b847-94605de78390 |
| Figure 5 - Fresh human colon samples – healthy | https://dcor.mpl.mpg.de/9a6439a2-0220-40cc-a61e-dd0407aeedc9 |
| Figure 5 - Fresh human colon samples – tumour | https://dcor.mpl.mpg.de/84a6f22c-1df4-4add-b3b5-a4efe3c0adb1 |
| Figure 5 - Fresh human lung samples – healthy | https://dcor.mpl.mpg.de/d8d247d7-b2f4-406c-b7c2-43770653a16d |
| Figure 5 - Fresh human lung samples – tumour | https://dcor.mpl.mpg.de/fb460cd1-e82e-4963-bc51-9bf83d3ea013 |
| Figure 5 – Frozen human colon - blind samples | https://dcor.mpl.mpg.de/342b1d2e-5e1d-47ed-88c2-7871243f739a |
| Figure 5 - Fresh human colon - blind samples | https://dcor.mpl.mpg.de/498112f0-b7b9-45cc-b71f-79e729bbfc30 |
| Figure 5 - Fresh human lung - blind samples | https://dcor.mpl.mpg.de/a3698039-e441-43fc-aa4d-67833d0ae942 |
| Extended Data Figure 3 - Cell doublets | https://dcor.mpl.mpg.de/96ade6cb-3d46-40fd-88b6-d9c59a9ae330 |
| Extended Data Figure 4 - Liver and lung | https://dcor.mpl.mpg.de/03c49f24-8d41-445b-aae3-a18790bfe82e |
| Extended Data Figure 5 - Comparison of fresh and frozen human colon | https://dcor.mpl.mpg.de/5cc528df-732f-4035-a99f-7f004ae3e37c |

**References**


1. Ruiz, V. E., Sachdev, M., Zhang, S., Wen, S. & Moss, S. F. Isolating, immunophenotyping and ex vivo stimulation of CD4+ and CD8+ gastric lymphocytes during murine Helicobacter pylori infection. *J. Immunol. Methods* **384**, 157–163 (2012).

2. Valente, M. J. *et al.* A Rapid and Simple Procedure for the Establishment of Human Normal and Cancer Renal Primary Cell Cultures from Surgical Specimens. *PLoS One* **6**, e19337 (2011).

3. Epshtein, A., Sakhneny, L. & Landsman, L. Isolating and Analyzing Cells of the Pancreas Mesenchyme by Flow Cytometry. *J. Vis. Exp.* 5–11 (2017) doi:10.3791/55344.

4. Soteriou, D. *et al.* Datasets for: Rapid single-cell physical phenotyping of mechanically dissociated tissue biopsies. *Deformability Cytometry Open Repository (DCOR)* https://dcor.mpl.mpg.de/organization/soteriou-kubankova (2023).